

On the derivation of a high-velocity tail from the Boltzmann–Fokker–Planck equation for shear flow

L. Acedo,* A. Santos,† and A. V. Bobylev†
(November 2, 2018)

Uniform shear flow is a paradigmatic example of a nonequilibrium fluid state exhibiting non-Newtonian behavior. It is characterized by uniform density and temperature and a linear velocity profile $U_x(y) = ay$, where a is the constant shear rate. In the case of a rarefied gas, all the relevant physical information is represented by the one-particle velocity distribution function $f(\mathbf{r}, \mathbf{v}) = f(\mathbf{V})$, with $\mathbf{V} \equiv \mathbf{v} - \mathbf{U}(\mathbf{r})$, which satisfies the standard nonlinear integro-differential Boltzmann equation. We have studied this state for a two-dimensional gas of Maxwell molecules with a collision rate $K(\theta) \propto \lim_{\epsilon \rightarrow 0} \epsilon^{-2} \delta(\theta - \epsilon)$, where θ is the scattering angle, in which case the nonlinear Boltzmann collision operator reduces to a Fokker–Planck operator. We have found analytically that for shear rates larger than a certain threshold value $a_{\text{th}} \simeq 0.3520\nu$ (where ν is an average collision frequency and a_{th}/ν is the real root of the cubic equation $64x^3 + 16x^2 + 12x - 9 = 0$) the velocity distribution function exhibits an algebraic high-velocity tail of the form $f(\mathbf{V}; a) \sim |\mathbf{V}|^{-4-\sigma(a)} \Phi(\varphi; a)$, where $\varphi \equiv \tan V_y/V_x$ and the angular distribution function $\Phi(\varphi; a)$ is the solution of a modified Mathieu equation. The enforcement of the periodicity condition $\Phi(\varphi; a) = \Phi(\varphi + \pi; a)$ allows one to obtain the exponent $\sigma(a)$ as a function of the shear rate. It diverges when $a \rightarrow a_{\text{th}}$ and tends to a minimum value $\sigma_{\text{min}} \simeq 1.252$ in the limit $a \rightarrow \infty$. As a consequence of this power-law decay for $a > a_{\text{th}}$, all the velocity moments of a degree equal to or larger than $2 + \sigma(a)$ are divergent. In the high-velocity domain the velocity distribution is highly anisotropic, with the angular distribution sharply concentrated around a preferred orientation angle $\tilde{\varphi}(a)$, which rotates from $\tilde{\varphi} = -\pi/4, 3\pi/4$ when $a \rightarrow a_{\text{th}}$ to $\tilde{\varphi} = 0, \pi$ in the limit $a \rightarrow \infty$.

KEY WORDS: Uniform shear flow; Boltzmann equation; Maxwell molecules; High-velocity tail.

I. INTRODUCTION

In the investigation of the physical properties of fluids far from equilibrium, one usually focuses on the nonlinear dependence of the momentum and heat fluxes on the gradients of the hydrodynamic fields. The associated transport properties are related to the population of molecules with energies of the order of or less than the mean kinetic energy, so that molecules moving with velocities much larger than the thermal velocity hardly contribute to those properties. However, the knowledge of the high-energy population in nonequilibrium states is important not only from a theoretical point of view but also because that population may play a crucial role in processes such as chemical reactions with a high activation energy or in the controlled thermonuclear fusion of a confined hydrogen plasma.

Of course, a general description of the high-energy population for arbitrary nonequilibrium states is not possible. Therefore, it is worthwhile gaining some insight by considering particular states. It can be fairly said that one of the most extensively studied nonequilibrium states is the so-called uniform shear flow (USF). At a macroscopic level, it is characterized by a constant density n , a uniform temperature T , and a linear profile of the x component of the flow velocity along the y direction, i.e., $U_x(y) = ay$, a being the constant shear rate. This shear rate represents the only control parameter needed to measure the departure of the USF state from equilibrium. At a microscopic level,¹ the USF is described by a solution of the Liouville equation with Lees-Edwards boundary conditions,² which can be seen as periodic boundary conditions in the *local* rest frame. These conditions assure the consistency of uniform shear, density, and temperature, even far from equilibrium. This state has been widely used to study rheological properties, such as shear thinning and viscometric effects. It must be borne in mind that, except in the linear regime, the USF is not equivalent to the planar Couette flow. In the latter, the shearing is produced by “realistic” walls in relative motion, so that the boundary conditions correspond to particles interacting with the walls rather than to the generalized periodic Lees-Edwards boundary conditions. In contrast to USF, boundary effects are present in the

*Departamento de Física, Universidad de Extremadura, E-06071 Badajoz, Spain

†Division of Engineering Sciences, Physics and Mathematics, Karlstad University, Karlstad, Sweden

Couette flow and, in addition, the shear rate, density, and temperature are local quantities.³ Far from equilibrium, the rheological properties of the Couette flow differ from those of the USF.⁴

In general, no rigorous theory based on first principles exists for the USF state. On the other hand, if one restricts oneself to the case of dilute gases, the most relevant physical information is contained in the one-particle velocity distribution function $f(\mathbf{r}, \mathbf{v}, t)$ and then the Liouville equation or, equivalently, the BBGKY hierarchy can be successfully contracted to a closed equation for f , namely the nonlinear Boltzmann equation.^{5,6} A number of exact results have been derived from the Boltzmann equation specialized to the case of Maxwell molecules under USF. Almost half a century ago, Ikenberry and Truesdell⁷⁻⁹ showed that the infinite hierarchy of moment equations could be recursively solved. In particular, they obtained the temporal evolution of the second-degree moments, which are the quantities related to the rheological properties, for arbitrary values of the shear rate. Truesdell and Muncaster⁹ analyzed the temporal evolution of the third-degree moments (for instance, the heat flux), which are expected to vanish for long times because of symmetry. They observed that for shear rates larger than a certain value some of those moments increased with time, a feature they referred to as an *instability* in the heat flux solution. However, further analysis¹⁰ has proved that such an increase is actually a consequence of the viscous heating and that the heat flux does indeed vanish for long times when it is properly scaled with respect to the thermal velocity, so the apparent instability is then removed. More recently, explicit expressions for the fourth-degree moments have also been derived.^{10,11} While the (scaled) second-degree moments remain finite for arbitrary shear rates, there exists a critical value a_c of the shear rate, beyond which the fourth-degree moments diverge. The analysis of this singular behavior has been extended to moments up to degree 36 and 240 for three-dimensional¹² and two-dimensional¹³ systems, respectively. These exact results show that the moments of an even degree $k \geq 4$ are divergent if the shear rate is larger than a certain k -dependent critical value that decreases as the degree k increases. This behavior of the moments indicates that the distribution function presents an algebraic high-velocity tail. This expectation has been strongly supported by direct Monte Carlo simulations,^{13,14} which also show that the high-velocity distribution function presents a strong anisotropy. To the best of our knowledge these high-velocity properties have not been so far confirmed at a theoretical level. The aim of this paper is to fill this gap.

Since, due to the complexity of the collision term, the nonlinear Boltzmann equation is extremely difficult to solve, we consider here a simplified model of two-dimensional Maxwell molecules. In this model the collision rate is assumed to vanish for all the scattering angles except for a small angle corresponding to grazing collisions. This allows us to replace the nonlinear collision operator by a Fokker-Planck operator⁵ that, on the other hand, preserves most of the general features of the original operator. By assuming a high-velocity tail of the form $f(\mathbf{V}) \sim V^{-4-\sigma} \Phi(\varphi)$, where $\mathbf{V} = \mathbf{v} - \mathbf{U}$ is the peculiar velocity and $\varphi = \tan^{-1} V_y/V_x$ is the polar angle in velocity space, the Boltzmann equation yields a linear second-order ordinary differential equation for Φ . The periodicity condition on $\Phi(\varphi)$ determines σ as a function of the shear rate, thus confirming the assumed algebraic tail. The results show that the exponent $\sigma(a)$ is a monotonically decreasing function that diverges when a approaches a threshold value a_{th} and tends to a minimum value $\sigma_{\text{min}} \simeq 1.252$ in the limit of large shear rates. The first property means that for shear rates smaller than a_{th} the distribution function decays for large velocities more rapidly than any power law (e.g., as a stretched exponential), while the second property implies that, even for large shear rates, all the moments of the form $\langle V^k \rangle$ with $k \leq 2 + \sigma_{\text{min}}$ are finite. The orientation distribution $\Phi(\varphi)$ in the high-velocity domain is concentrated around a preferred angle $\tilde{\varphi}(a)$ that rotates counter-clockwise as the shear rate increases. Moreover, this distribution is infinitely sharp for the extreme values of the shear rate: $\lim_{a \rightarrow a_{\text{th}}} \Phi(\varphi) = \frac{1}{2}[\delta(\varphi - 3\pi/4) + \delta(\varphi - 7\pi/4)]$, $\lim_{a \rightarrow \infty} \Phi(\varphi) = \frac{1}{2}[\delta(\varphi) + \delta(\varphi - \pi)]$. To our knowledge, this is the first time that such a detailed picture of the high-velocity behavior of the solution to the Boltzmann equation in a far from equilibrium state has been analytically described.

The organization of this paper is as follows. The uniform shear flow state is described in Sec. II. Some exact scaling properties in the case of Maxwell molecules are used to map the time-dependent state of the system onto an equivalent “thermostatted” state which reaches a nonequilibrium steady state for long times. The simple scattering model representing grazing collisions is introduced in Sec. III. The temporal evolution of the (scaled) fourth-degree moments is analyzed, the results showing that they diverge for shear rates equal to or larger than a certain critical value a_c , as expected from previous analyses for more realistic scattering laws.^{13,14} The derivation of the high-velocity tail of the form $f(\mathbf{V}) \sim V^{-4-\sigma} \Phi(\varphi)$ is worked out in Sec. IV, where the dependence of the exponent σ on the shear rate is obtained from the periodicity condition $\Phi(\varphi) = \Phi(\varphi + \pi)$. Finally, the results are discussed in Sec. V.

II. UNIFORM SHEAR FLOW

The most relevant quantity to determine the nonequilibrium properties of a dilute gas is the one-particle velocity distribution function $f(\mathbf{r}, \mathbf{v}, t)$. Its time evolution is governed by the nonlinear Boltzmann equation. In the absence of external forces, it reads:^{5,6,15}

$$\begin{aligned} \frac{\partial}{\partial t} f + \mathbf{v} \cdot \frac{\partial}{\partial \mathbf{r}} f &= \int d\mathbf{v}_1 \int d\Omega |\mathbf{v} - \mathbf{v}_1| I(|\mathbf{v} - \mathbf{v}_1|, \theta) (f' f'_1 - f f_1) \\ &\equiv Q[f, f], \end{aligned} \quad (1)$$

where $I(g, \theta)$ is the differential cross section (θ being the scattering angle) and we are using standard notation to denote the distribution function evaluated at pre- and post-collisional velocities. Of course, Eq. (1) must be supplemented with the appropriate initial and boundary conditions.

Let us now introduce the velocity field

$$U_i(\mathbf{r}) = a_{ij} r_j, \quad a_{ij} = a \delta_{ix} \delta_{jy}, \quad (2)$$

where a is a constant shear rate. We define the uniform shear flow (USF) state as the one that is spatially homogeneous when the velocities of particles are referred to a Lagrangian frame moving with the velocity field $\mathbf{U}(\mathbf{r})$, i.e.,

$$f(\mathbf{r}, \mathbf{v}, t) = f(\mathbf{V}, t), \quad (3)$$

where $\mathbf{V} \equiv \mathbf{v} - \mathbf{U}(\mathbf{r})$ is the peculiar velocity. Consequently, the Boltzmann equation (1) becomes

$$\frac{\partial}{\partial t} f - \frac{\partial}{\partial V_i} a_{ij} V_j f = Q[f, f]. \quad (4)$$

The usual boundary conditions used to generate the USF are the Lees-Edwards periodic boundary conditions,^{2,16} but the so-called ‘‘bounce-back’’ boundary conditions^{17,18} are also consistent with the USF. It is worthwhile noting that Eq. (4) can be interpreted as representing a *homogeneous* state under the action of the nonconservative external force $F_i = -m a_{ij} V_j$. Note also that Eq. (4) is invariant under the transformation $(V_x, V_y) \rightarrow (-V_x, -V_y)$.

Let us now particularize to the case of Maxwell molecules, i.e., particles interacting via a potential $\phi(r) \propto r^{-2(d-1)}$, where d is the dimensionality of the system. In that case, the collision rate $gI(g, \theta) = K(\theta)$ is independent of the relative velocity g .^{19,20} From a mathematical point of view, this makes the Boltzmann collision operator more tractable than for other interaction models. In particular, any collisional moment of degree k can be expressed as a bilinear combination of moments of f of degrees k' and k'' , such that $k' + k'' = k$.^{9,20,21} This allows one, in principle, to solve recursively the hierarchy of moment equations arising from Eq. (4), even though the explicit form for f is not known.^{7-14,22} In addition, Eq. (4) for Maxwell molecules exhibits the following scaling property.^{10,16} Let us introduce the scaled quantities

$$\bar{\mathbf{V}} = e^{-\alpha t} \mathbf{V}, \quad (5)$$

$$\bar{f}(\bar{\mathbf{V}}, t) = e^{d\alpha t} f(\mathbf{V}, t), \quad (6)$$

where α is an *arbitrary* constant. Then, Eq. (4) reduces to

$$\frac{\partial}{\partial t} \bar{f} - \frac{\partial}{\partial \bar{V}_i} (a_{ij} \bar{V}_j + \alpha \bar{V}_i) \bar{f} = Q[\bar{f}, \bar{f}]. \quad (7)$$

This equation can be interpreted as the one corresponding to USF in presence of an external drag force $-m\alpha\bar{\mathbf{V}}$. Since the mapping of Eq. (4) onto Eq. (7) (and vice versa) is an exact property, we are free to choose the parameter α as we like. For convenience, we choose α as a function of the shear rate a by the condition that the scaled temperature

$$\bar{T}(t) = e^{-2\alpha t} T(t) = \frac{m}{3nk_B} \int d\bar{\mathbf{V}} \bar{\mathbf{V}}^2 \bar{f}(\bar{\mathbf{V}}, t) \quad (8)$$

reaches a constant value in the long-time limit. In the above equation, m is the mass of a particle, k_B is the Boltzmann constant, n is the number density, and T is the unscaled temperature. With this choice of α , the term $-m\alpha\bar{\mathbf{V}}$ plays the role of a *thermostat* force. This kind of thermostat forces is usually employed in nonequilibrium molecular dynamics simulations.²³⁻²⁵ Henceforth, we will adopt the point of view behind Eq. (7), i.e., all the quantities will be understood to be scaled quantities, and we will drop the bars for convenience. Taking second-degree moments in Eq. (7) we have

$$\frac{\partial}{\partial t} P_{ij} + (a_{ik} P_{jk} + a_{jk} P_{ik}) + 2\alpha P_{ij} = -\nu (P_{ij} - p\delta_{ij}), \quad (9)$$

where

$$P_{ij} = m \int d\mathbf{V} V_i V_j f \quad (10)$$

is the pressure tensor, $p = nk_B T = \frac{1}{d} \text{Tr} \mathbf{P}$ is the hydrostatic pressure, and ν is an effective collision frequency defined as (see Appendix A)

$$\nu = n \frac{2d}{d-1} \int d\Omega K(\theta) \sin^2 \frac{\theta}{2} \cos^2 \frac{\theta}{2}. \quad (11)$$

It is convenient to choose ν^{-1} as the time unit and introduce the dimensionless quantities $t^* = \nu t$, $a^* = a/\nu$, and $\alpha^* = \alpha/\nu$. Henceforth, these reduced variables will be implicitly assumed and the asterisks will be omitted.

From Eq. (9) it is easy to get the following closed differential equation for the temperature:

$$\left(\frac{\partial}{\partial t} + 2\alpha \right) \left(\frac{\partial}{\partial t} + 2\alpha + 1 \right)^2 T = \frac{2}{d} a^2 T. \quad (12)$$

So far, α is arbitrary. Now, as said before, we choose α under the condition that the temperature reaches a stationary value in the long-time limit. This implies that $\alpha(a)$ is the real root of the cubic equation

$$a^2 = d\alpha(1 + 2\alpha)^2, \quad (13)$$

i.e.,

$$\begin{aligned} \alpha(a) &= \frac{2}{3} \sinh^2 \left[\frac{1}{6} \cosh^{-1}(1+z) \right] \\ &= \frac{1}{6} \left(1+z + \sqrt{2z+z^2} \right)^{1/3} + \frac{1}{6} \left(1+z - \sqrt{2z+z^2} \right)^{1/3} - \frac{1}{3}, \end{aligned} \quad (14)$$

where $z \equiv \frac{27}{d} a^2$. The stationary values of the elements of the pressure tensor are then easily obtained from Eq. (9):

$$P_{xx} = p \frac{1+2d\alpha}{1+2\alpha}, \quad P_{yy} = \dots = P_{dd} = \frac{p}{1+2\alpha}, \quad P_{xy} = -a \frac{p}{(1+2\alpha)^2}. \quad (15)$$

These quantities exhibit non-Newtonian effects: normal stress differences and a nonlinear relationship between the shear stress and the shear rate.

While the second-degree moments are well defined for any value of the shear rate a , moments of degree four and higher diverge if a is larger than a certain critical value a_c .^{10–13} This suggests that the stationary solution to Eq. (7) presents a high-velocity tail of the form $f(\mathbf{V}) \sim V^{-d-2-\sigma(a)}$, where $\sigma(a)$ is a positive definite exponent that is a decreasing function of the shear rate.

III. A SIMPLE SCATTERING MODEL

In the Monte Carlo simulations as well as in the theoretical analysis of higher-degree moments presented in Ref. 13 the scattering law was assumed to be isotropic: $K(\theta) = \text{const}$. However, this choice for the collision rate does not simplify the collision operator in a significant way as to allow one to confirm theoretically the high-velocity tail. Since the main features can be expected to be to some extent independent of the particular scattering model $K(\theta)$, it is convenient to consider the simplest choice lending itself to an analytic or semi-analytic treatment. Here we consider the following simplified scattering model:

$$K(\theta) = K_0 \lim_{\epsilon \rightarrow 0} \epsilon^{-d} \delta(\theta - \epsilon), \quad (16)$$

which corresponds to grazing collisions of Maxwell molecules. It is proved in Appendix B that in this case the collision operator becomes

$$Q[f, f] \rightarrow \frac{\nu}{4d} \left[(d-1) \frac{\partial}{\partial V_i} V_i + \frac{dp\delta_{ij} - P_{ij}}{mn} \frac{\partial}{\partial V_i} \frac{\partial}{\partial V_j} + \mathcal{L}^2 \right] f(\mathbf{V}), \quad (17)$$

where

$$\mathcal{L}^2 = \left(\mathbf{V} \times \frac{\partial}{\partial \mathbf{V}} \right)^2 = \frac{\partial}{\partial V_i} (V^2 \delta_{ij} - V_i V_j) \frac{\partial}{\partial V_j}. \quad (18)$$

The right-hand side of (17) has the structure of a Fokker–Planck operator with a velocity-dependent diffusion term. The model (17) was derived (with $d = 3$) in Section II.9 of Ref. 5 as the contribution of grazing collisions to the collision operator. Since here only grazing collisions are considered, the above contribution becomes the entire collision operator.

Now, we restrict ourselves to the two-dimensional case ($d = 2$), so that Eq. (7) becomes

$$\frac{\partial}{\partial t} f - a V_y \frac{\partial}{\partial V_x} f - \alpha \frac{\partial}{\partial V_i} V_i f = \frac{1}{8} \left(\frac{\partial}{\partial V_i} V_i + \frac{2p\delta_{ij} - P_{ij}}{mn} \frac{\partial}{\partial V_i} \frac{\partial}{\partial V_j} + \mathcal{L}^2 \right) f, \quad (19)$$

where we have already made $\nu = 1$. Of course, by taking second-degree moments we reobtain Eq. (9). Let us consider now the fourth-degree moments

$$M_s = \frac{1}{n} \int d\mathbf{V} V_x^{4-s} V_y^s f(\mathbf{V}), \quad s = 0, \dots, 4. \quad (20)$$

Multiplying both sides of Eq. (19) by $V_x^{4-s} V_y^s$ and integrating over \mathbf{V} we get

$$\begin{aligned} \frac{\partial}{\partial t} M_s + (4-s)aM_{s+1} + 4\alpha M_s &= -\frac{4+s(4-s)}{4} M_s + \frac{(4-s)(3-s)}{8} M_{s+2} + \frac{s(s-1)}{8} M_{s-2} \\ &\quad - \frac{s(4-s)}{4} P_1 P_{s-1} + \frac{(4-s)(3-s)}{8} P_2 P_s + \frac{s(s-1)}{8} P_0 P_{s-2}, \end{aligned} \quad (21)$$

where $P_0 \equiv P_{xx}/mn$, $P_1 \equiv P_{xy}/mn$, and $P_2 \equiv P_{yy}/mn$. In matrix notation,

$$\frac{\partial}{\partial t} M_s = - \sum_{s'=0}^4 \Lambda_{ss'} M_{s'} + N_s, \quad (22)$$

where

$$\Lambda_{ss'}(a) = \left[4\alpha(a) + \frac{4+s(4-s)}{4} \right] \delta_{s',s} + (4-s)a\delta_{s',s+1} - \frac{(4-s)(3-s)}{8} \delta_{s',s+2} - \frac{s(s-1)}{8} \delta_{s',s-2}, \quad (23)$$

and N_s is a bilinear combination of second-degree moments. The temporal evolution of the moments M_s is governed by the eigenvalues $\lambda_s(a)$ of the matrix $\Lambda_{s,s'}(a)$. At equilibrium ($a = 0$) the eigenvalues are $\lambda_0(0) = \frac{1}{2}$, $\lambda_1(0) = \lambda_2(0) = 1$, and $\lambda_3(0) = \lambda_4(0) = \frac{5}{2}$. At finite shear rate, the degeneracy is broken, (λ_1, λ_2) and (λ_3, λ_4) becoming two conjugate pairs. The trace of the matrix $\Lambda_{s,s'}(a)$ is $\lambda_0(a) + 2\text{Re}\lambda_1(a) + 2\text{Re}\lambda_3(a) = \frac{15}{2} + 20\alpha(a)$, which is a monotonically increasing function of the shear rate. On the other hand, as Fig. 1 shows, while the real parts of λ_1 – λ_4 monotonically increase with the shear rate, the only real eigenvalue λ_0 decreases and eventually becomes negative for $a \geq a_c \simeq 2.48553$. This implies that for $a \geq a_c$ the fourth-degree moments diverge in the long-time limit. Of course, moments of a degree higher than four are also divergent for $a \geq a_c$. As said in the Introduction, the existence of a critical shear rate a_c was first obtained analytically in the case of Maxwell molecules with regular collision rates, both for $d = 3$ ^{10–12} and $d = 2$.^{13,14} For instance, $a_c \simeq 5.847$ ¹³ in the case of two-dimensional Maxwell molecules with isotropic scattering. Thus, the singular behavior of the fourth-degree moments M_s is not an artifact of the scattering model (16).

The divergence of M_s for $a \geq a_c$ is a strong indication that the velocity distribution function reaches a steady state form that has an algebraic decay $f(\mathbf{V}) \sim V^{-4-\sigma(a)}$ with $\sigma(a) \leq 2$. Conversely, for $a < a_c$ one can expect that $\sigma(a) > 2$, so that the fourth-degree moments converge, but moments of a higher degree $2k + 2$ will diverge whenever the shear rate is such that $\sigma(a) \leq 2k$. While this scenario has been supported by computer simulations,^{13,14} we are not aware of any derivation of this high-velocity tail from the Boltzmann equation, prior to the one presented in the next Section.

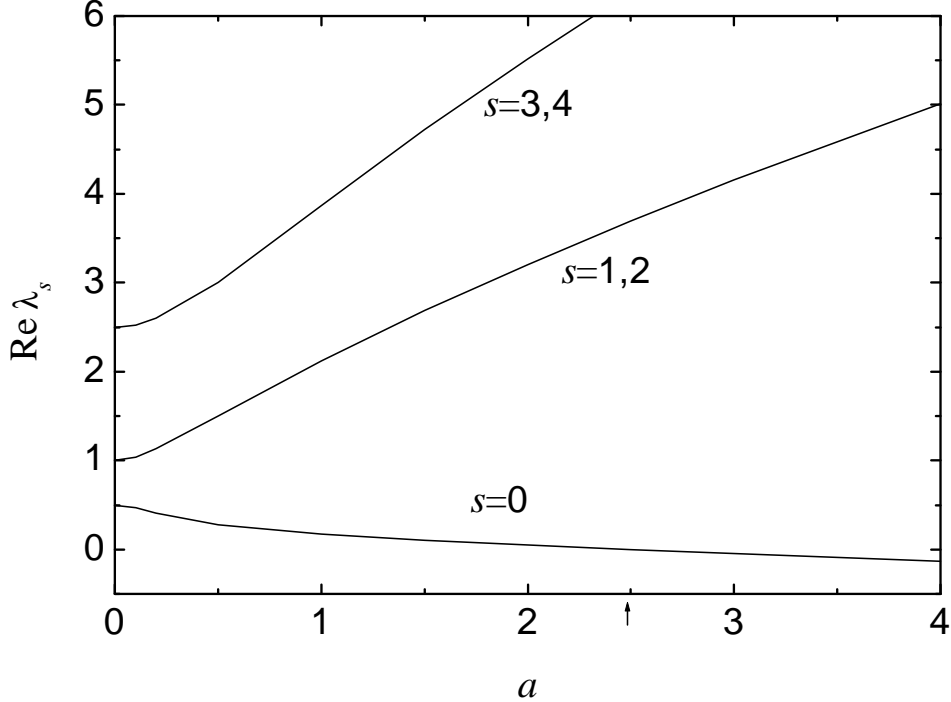


FIG. 1. Real parts of the eigenvalues λ_s associated with the fourth-degree moments, as functions of the shear rate. The arrow indicates the location of the critical shear rate $a_c \simeq 2.48553$ beyond which $\lambda_0 < 0$ and, consequently, all the moments of degree four and higher diverge.

IV. HIGH-VELOCITY TAIL

From Eq. (19) we get the following equation for the steady state distribution function:

$$\left[8aV_y \frac{\partial}{\partial V_x} + (1 + 8\alpha) \frac{\partial}{\partial V_i} V_i + \mathcal{L}^2 \right] f = \frac{P_{ij} - 2p\delta_{ij}}{mn} \frac{\partial}{\partial V_i} \frac{\partial}{\partial V_j} f. \quad (24)$$

This is still a complicated equation to solve for all velocities. However, we are interested here in the solution for large velocities. In that domain, the right-hand side of Eq. (24) is of order V^{-2} relative to the term $\mathcal{L}^2 f$ [cf. Eq. (18)], so it can be neglected. By the arguments given at the end of the previous Section, we look for self-consistent solutions with the asymptotic behavior

$$f(\mathbf{V}; a) \sim V^{-4-\sigma(a)} \Phi(\varphi; a) \quad (25)$$

for large velocities. In Eq. (25) φ is the polar angle in velocity space, i.e.,

$$V_x = V \cos \varphi, \quad V_y = V \sin \varphi, \quad (26)$$

Φ is a function measuring the degree of anisotropy of the high-velocity distribution function, and σ is the exponent characterizing the algebraic decay. These two quantities must be determined self-consistently. According to Eq. (25), the left-hand side of Eq. (24) is proportional to $V^{-4-\sigma}$, while the right-hand side is proportional to $V^{-6-\sigma}$. Consequently, the latter must be neglected against the former in the limit of large velocities, as said before.

In polar coordinates, the operators on the left-hand side of Eq. (24) become

$$V_y \frac{\partial}{\partial V_x} = \cos \varphi \sin \varphi V \frac{\partial}{\partial V} - \sin^2 \varphi \frac{\partial}{\partial \varphi}, \quad (27)$$

$$\frac{\partial}{\partial V_i} V_i = 2 + V \frac{\partial}{\partial V}, \quad (28)$$

$$\mathcal{L}^2 = \frac{\partial^2}{\partial \varphi^2}. \quad (29)$$

Thus, when Eq. (25) is inserted into Eq. (24) one gets the following linear second-order ordinary differential equation

$$\Phi''(\varphi) - p[1 - \cos(2\varphi)]\Phi'(\varphi) - [\beta + 2q \sin(2\varphi)]\Phi(\varphi) = 0, \quad (30)$$

where $p \equiv 4a$, $\beta \equiv (2 + \sigma)(1 + 8\alpha)$, and $q \equiv 2a(4 + \sigma)$. Equation (30) is a generalization of Mathieu's equation^{26,27} and reduces to it if $p = 0$. However, since in our case $p \neq 0$, we have to deal with Eq. (30) rather than with Mathieu's well-known equation. The symmetry property $f(\mathbf{V}) = f(-\mathbf{V})$ implies the periodicity condition $\Phi(\varphi) = \Phi(\varphi + \pi)$. From a mathematical point of view, Eq. (30) supports those periodic solutions provided that the parameter β takes a characteristic value $\beta(p, q)$. Since the shear rate a and the scaling coefficient α are related through Eqs. (13) and (14), only two of the three parameters β , p , and q are independent. Thus, the characteristic value $\beta(p, q)$ translates into $\sigma(a)$. In case there are multiple solutions for a given a , the relevant solution is the one related to the dominant tail, which corresponds to the smallest value of σ . In the subsequent mathematical analysis we consider β , p , and q as independent parameters and only at the end we will take into account that in our physical problem $\beta = (2 + \sigma)(1 + 8\alpha)$, $p = 4a$, and $q = 2a(4 + \sigma)$.

In order to find the periodic solutions to Eq. (30) and the corresponding characteristic values, we write

$$\Phi(\varphi) = \sum_{m=-\infty}^{\infty} C_m e^{2im\varphi}, \quad C_{-m} = C_m^*. \quad (31)$$

If the above is substituted into Eq. (30), one obtains the recurrence relations

$$\mu_{m+1}C_{m+1} + \gamma_m C_m - \mu_{-m+1}C_{m-1} = 0, \quad (32)$$

where

$$\mu_m \equiv q - mp, \quad \gamma_m \equiv 2mp - i(\beta + 4m^2). \quad (33)$$

In particular, setting $m = 0$,

$$C_0 = -i \frac{q-p}{\beta} (C_1 - C_{-1}) = 2 \frac{q-p}{\beta} \text{Im}C_1. \quad (34)$$

Therefore, by applying Eq. (32) to $m \geq 1$, all the coefficients C_m , $m \geq 2$, can be obtained recursively from C_1 . The coefficients C_m with $m \leq -2$ are then given by the symmetry relation $C_{-m} = C_m^*$. The characteristic values arise from the convergence condition

$$\lim_{m \rightarrow \infty} |D_m| < 1, \quad D_m \equiv \frac{C_{m+1}}{C_m}. \quad (35)$$

The recurrence relation for the ratios D_m is

$$\mu_{m+1}D_m + \gamma_m - \mu_{-m+1}D_{m-1}^{-1} = 0. \quad (36)$$

Thus, all the coefficients D_m with $m \geq 1$ are obtained from D_0 , the latter being subject to the compatibility condition

$$\text{Im}D_0 = \frac{\beta}{2(q-p)}, \quad (37)$$

as follows from Eq. (34). Equation (36) shows that there are two possible asymptotic behaviors of D_m for large m . Either

$$D_m \approx -\frac{4i}{p}m \quad (38)$$

or

$$D_m \approx -\frac{p}{4i}m^{-1}. \quad (39)$$

The latter is the only one consistent with the convergence condition (35). This allows us to use (36) to develop D_m as the continued fraction

$$D_m = \frac{\mu_{-m}}{\gamma_{m+1} + \mu_{m+2} D_{m+1}} \quad (40a)$$

$$= \frac{\mu_{-m}}{\gamma_{m+1} +} \frac{\mu_{m+2} \mu_{-m-1}}{\gamma_{m+2} +} \frac{\mu_{m+3} \mu_{-m-2}}{\gamma_{m+3} +} \dots \quad (40b)$$

Finally, the characteristic values are obtained from the compatibility condition (37), namely

$$\text{Im} \left(\frac{\mu_0}{\gamma_1 +} \frac{\mu_2 \mu_{-1}}{\gamma_2 +} \frac{\mu_3 \mu_{-2}}{\gamma_3 +} \dots \right) = \frac{\beta}{2(q-p)}. \quad (41)$$

Once the relationship $\beta(p, q)$ is found, the ratios D_m are obtained from Eq. (40b) or, equivalently, from Eq. (40a) for $m = 0$ and from Eq. (36) for $m \geq 1$. The angular distribution function is then given by Eq. (31) with

$$C_m = \frac{1}{2\pi} \prod_{m'=0}^{m-1} D_{m'}, \quad m \geq 1, \quad (42)$$

where the particular value $C_0 = 1/2\pi$ has been chosen to verify the normalization condition

$$\int_0^{2\pi} d\varphi \Phi(\varphi) = 1. \quad (43)$$

Since Eqs. (40b) and (41) involve infinite continued fractions, in practice we proceed by setting $D_N = -(p/4i)N^{-1}$ for a certain large value of N and then using (40a) to get D_m for $m \leq N - 1$ up to $m = 0$. We have typically taken $N \sim 10^3$ and have checked that the results are rather insensitive to a further increase of N .

Before going back to our original physical problem and take into account the expressions of β , p , and q in terms of a and σ , it is worthwhile exploring the following limiting cases.

- (i) Consider first that the ratio q/p is equal to an integer number, $q/p = k + 2$. This means that $\mu_{k+2} = 0$, so that Eq. (41) becomes

$$\text{Im} \left(\frac{\mu_0}{\gamma_1 +} \frac{\mu_2 \mu_{-1}}{\gamma_2 +} \frac{\mu_3 \mu_{-2}}{\gamma_3 +} \dots \frac{\mu_{k+1} \mu_{-k}}{\gamma_{k+1} +} \right) = \frac{\beta}{2(k+1)p}, \quad (44)$$

which gives rise to an algebraic equation of degree $2k + 3$ for β . For instance,

$$\beta^3 + 8\beta^2 + 16\beta - 16p^2 = 0, \quad (45)$$

$$\beta^5 + 40\beta^4 + 528\beta^3 + 16(160 - 21p^2)\beta^2 + 256(16 - 15p^2)\beta - 12288p^2 = 0, \quad (46)$$

for $k = 0$ and $k = 1$, respectively. Next, Eq. (40a) gives D_m for $m \leq k$ in a closed form, while the infinite continued fraction (40b) must be used for $m \geq k + 1$. For instance, in the case $k = 0$,

$$D_1 = \frac{4p}{4p - (16 + \beta)i}, \quad D_0 = 3p \frac{4p - (16 + \beta)i}{12p^2 - (4 + \beta)(16 + \beta) - 6p(8 + \beta)i}. \quad (47)$$

- (ii) We now consider the limit $q \rightarrow \infty$ with $p = \text{finite}$. In that case, as verified later by consistency, the characteristic value scales as $\beta \rightarrow q\beta_1$, so that $\mu_m \rightarrow q$ and $\gamma_m \rightarrow -iq\beta_1$. Consequently, Eq. (36) becomes

$$D_m - i\beta_1 - D_{m-1}^{-1} = 0. \quad (48)$$

The solution consistent with the convergence of the series and with Eq. (37) is simply $D_m = e^{-2i\varphi_0}$, where φ_0 is an angle defined by

$$\sin 2\varphi_0 = -\frac{\beta_1}{2}. \quad (49)$$

This implies that $0 \leq \beta_1 \leq 2$. The function Φ is

$$\begin{aligned}\Phi(\varphi) &= \frac{1}{2\pi} \sum_{m=-\infty}^{\infty} e^{2im(\varphi-\varphi_0)} \\ &= \frac{1}{2} [\delta(\varphi - \varphi_0) + \delta(\varphi - \varphi_0 + \pi)].\end{aligned}\quad (50)$$

(iii) As a third limiting case, let us consider $q \rightarrow \infty$, $p \rightarrow \infty$, $q/p = \text{finite}$. It is then expected that $\beta/q \rightarrow 0$, so that $\gamma_m \rightarrow 2mp$. The consistent solution to Eq. (36) is $D_m = 1$, which corresponds to

$$\Phi(\varphi) = \frac{1}{2} [\delta(\varphi) + \delta(\varphi - \pi)].\quad (51)$$

Numerical analysis shows that in this limit the characteristic value β scales as $\beta = (\beta_2 p^2)^{1/3}$, where β_2 depends on the ratio q/p . In the special case of $q/p = \text{integer}$, the values of β_2 can be obtained from the algebraic equation (44). In particular, we get $\beta_2 = 16$, $\beta_2 = 336$, and $\beta_2 = 1008 \pm 96\sqrt{79}$ for $q/p = 2$, $q/p = 3$, and $q/p = 4$, respectively.

Now we apply the above analysis to the physical values $\beta = (2 + \sigma)(1 + 8\alpha)$, $p = 4a$, and $q = 2a(4 + \sigma)$, where a and α are related by Eqs. (13) and (14). The case (i) above, namely $q/p = k + 2$ with k integer, corresponds to $\sigma = 2k$, so that the solution to Eq. (44) gives the critical value of the shear rate beyond which all the moments of a degree equal to or larger than $2k + 2$ diverge. For $k = 0$, Eq. (45) gives rise to a cubic equation in α with no positive real root. This is expected since, as seen in Sec. II, the second-degree moments converge. For $k = 1$, Eq. (46) gives rise to the same quintic equation as obtained from $\det \Lambda_{ss'} = 0$, where the matrix $\Lambda_{ss'}$ is given by Eq. (23). The solution to this equation is $\alpha \simeq 0.61796$, which corresponds to $a \simeq 2.48553$, i.e., the critical value a_c found in Sec. II from the time evolution of the fourth-degree moments. In a similar way, we find the values $a \simeq 1.11175$, $a \simeq 0.87611$, $a \simeq 0.77052$, and $a \simeq 0.70842$ for $\sigma = 4$, $\sigma = 6$, $\sigma = 8$, and $\sigma = 10$, respectively. It is interesting to note that for $\sigma = 8$ and $\sigma = 10$ there exists a larger second solution ($a \simeq 52.5$ and $a \simeq 7.3$, respectively). This indicates that, in addition to the smallest eigenvalue, another of the eigenvalues governing the time evolution of the moments of degree 10 and 12, respectively, becomes negative at those large shear rates. This property has been observed before in the case of more realistic scattering laws.¹³ Of course, whenever there are different values of a consistent with a given value of σ , the actual function $\sigma(a)$ corresponds to the smallest value of a . Equivalently, if the characteristic equation (41) gives more than a value of σ for a given shear rate, the function $\sigma(a)$ is defined by the smallest value.

Now we consider the case (ii) above, which corresponds to the situation $\sigma \rightarrow \infty$. For which value of the shear rate does this happen? Mathematically speaking, there are an infinite number of solutions, namely the solutions to $(1 + 8\alpha)/2a = \beta_1$ with $0 \leq \beta_1 \leq 2$. Taking into account Eq. (13), this is equivalent to the cubic equation

$$8\beta_1^3 a^3 + 4(5\beta_1^2 - 16)a^2 + 6\beta_1 a - 9 = 0.\quad (52)$$

The real solution to this equation is a monotonically decreasing function of β_1 . Therefore, the physical value of the shear rate at which $\sigma \rightarrow \infty$ corresponds to $\beta_1 = 2$. This defines the threshold shear rate $a_{\text{th}} = (\sqrt{57}/96 + 67/864)^{1/3} - (\sqrt{57}/96 - 67/864)^{1/3} - 1/12 \simeq 0.352047$ beyond which the high-velocity tail has the form (25). Conversely, if $a \leq a_{\text{th}}$, the decay of the velocity distribution function is more rapid than any algebraic tail and *all* the velocity moments are convergent. This is in contrast with the results obtained from realistic scattering laws, which suggest that $a_{\text{th}} \rightarrow 0$ in those cases.^{12,13} Since $\beta_1 = 2$, Eq. (49) yields $\varphi_0 = 3\pi/4$ and Eq. (50) becomes

$$\lim_{a \rightarrow a_{\text{th}}} \Phi(\varphi; a) = \frac{1}{2} \left[\delta\left(\varphi - \frac{3}{4}\pi\right) + \delta\left(\varphi - \frac{7}{4}\pi\right) \right], \quad \lim_{a \rightarrow a_{\text{th}}} \sigma(a) = \infty.\quad (53)$$

Next, we investigate the limit of large shear rates, $a \rightarrow \infty$. In that case, $\alpha \approx a^{2/3}/2$, on account of Eq. (13). The question now is, what is the corresponding value $\sigma(\infty) \equiv \sigma_{\text{min}}$? Computer simulations for Maxwell molecules interacting with an isotropic scattering law suggest that $\sigma_{\text{min}} = 0$. However, this is not the case with the scattering law (16). According to the case (iii) above, the value of σ_{min} must be such that $\beta_2 = 4(2 + \sigma_{\text{min}})^3$ for $q/p = 2 + \sigma_{\text{min}}/2$. A numerical calculation gives $\sigma \simeq 1.252$, i.e., $\beta_2 \simeq 137.6$ at $q/p = 2.626$, which is consistent with the fact that $\beta_2 = 16$ and $\beta_2 = 336$ at $q/p = 2$ and $q/p = 3$, respectively. The minimum value σ_{min} means that, no matter how large the shear rate is, not only the second-degree moments are finite, but so are moments of the form $\langle V^k \rangle$ with $k \leq 2 + \sigma_{\text{min}} \simeq 3.252$. On the other hand, the high-velocity distribution function becomes strongly anisotropic for large shear rates since, according to Eq. (51),

$$\lim_{a \rightarrow \infty} \Phi(\varphi; a) = \frac{1}{2} [\delta(\varphi) + \delta(\varphi - \pi)], \quad \lim_{a \rightarrow \infty} \sigma(a) = \sigma_{\min}. \quad (54)$$

The complete dependence of σ on the shear rate is shown in Fig. 2, where the dotted lines indicate the locations of a_{th} and σ_{\min} . The region near $a = a_{\text{th}}$ is shown in Fig. 3. The results can be well fitted to the power law $\sigma \approx e^{-0.02}(a - a_{\text{th}})^{-1.93}$. The behavior for large shear rates is shown in Fig. 4, where the results can be fitted to $\sigma - \sigma_{\min} \approx e^{-0.04}a^{-0.71}$.

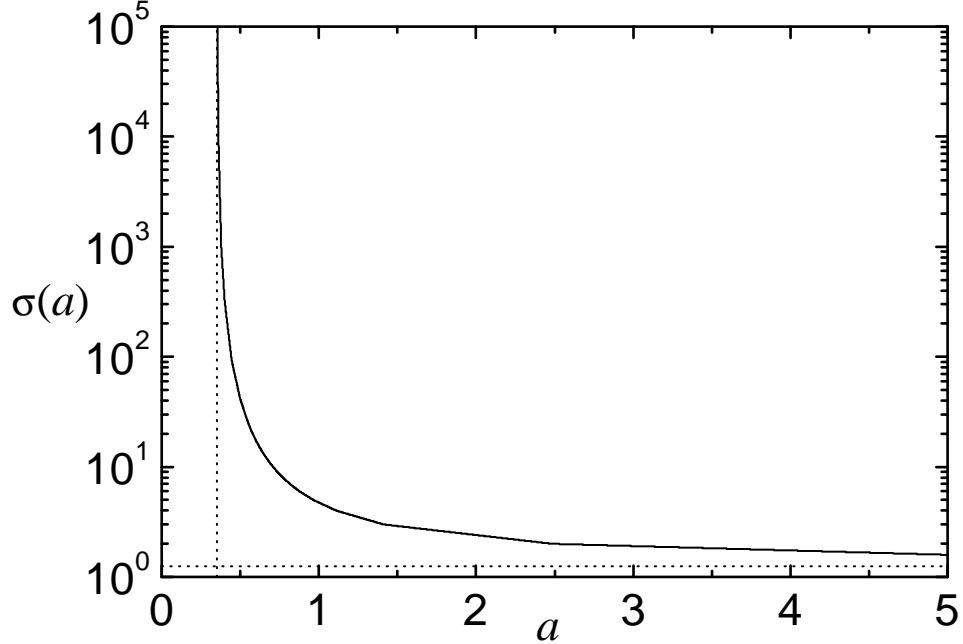


FIG. 2. Plot of the exponent σ as a function of the shear rate a . The vertical and horizontal dotted lines indicate the locations of $a_{\text{th}} \simeq 0.3520$ and $\sigma_{\min} \simeq 1.252$, respectively.

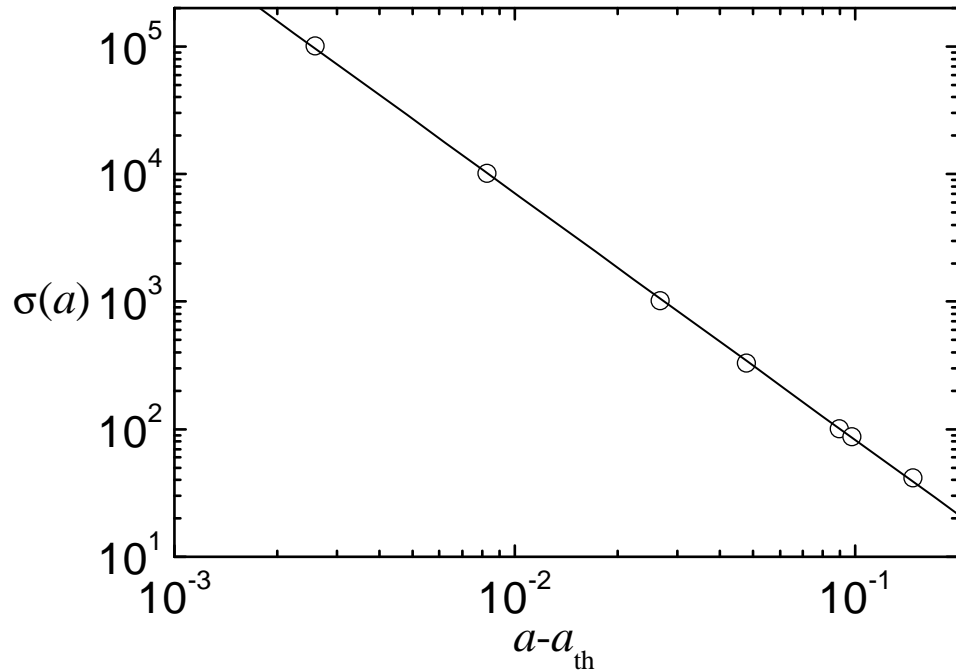


FIG. 3. Log-log plot of σ versus $a - a_{\text{th}}$. The solid line is a linear fit.

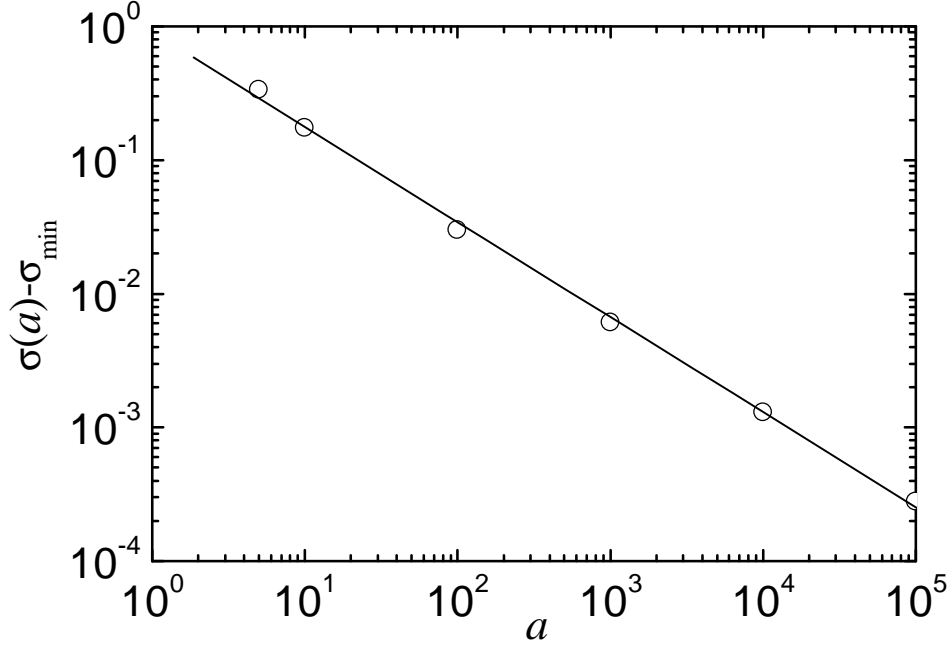


FIG. 4. Log-log plot of $\sigma - \sigma_{\min}$ versus a . The solid line is a linear fit.

In addition to the function $\sigma(a)$, the solution to the problem gives the angular distribution $\Phi(\varphi; a)$ for any shear rate $a > a_{\text{th}}$. The results indicate that in the high-velocity domain the distribution is highly anisotropic, with the angular distribution sharply concentrated around a preferred orientation angle $\tilde{\varphi}(a)$ that rotates from $\tilde{\varphi} = 3\pi/4, 7\pi/4$ when $a \rightarrow a_{\text{th}}$, Eq. (53), to $\tilde{\varphi} = 0, \pi$ when $a \rightarrow a_{\infty}$, Eq. (54). This transition is illustrated in Fig. 5. The anisotropic behavior observed in Fig. 5 is consistent with the one shown in Fig. 8 of Ref. 13 in the case of computer simulations of Maxwell molecules with a constant collision rate.

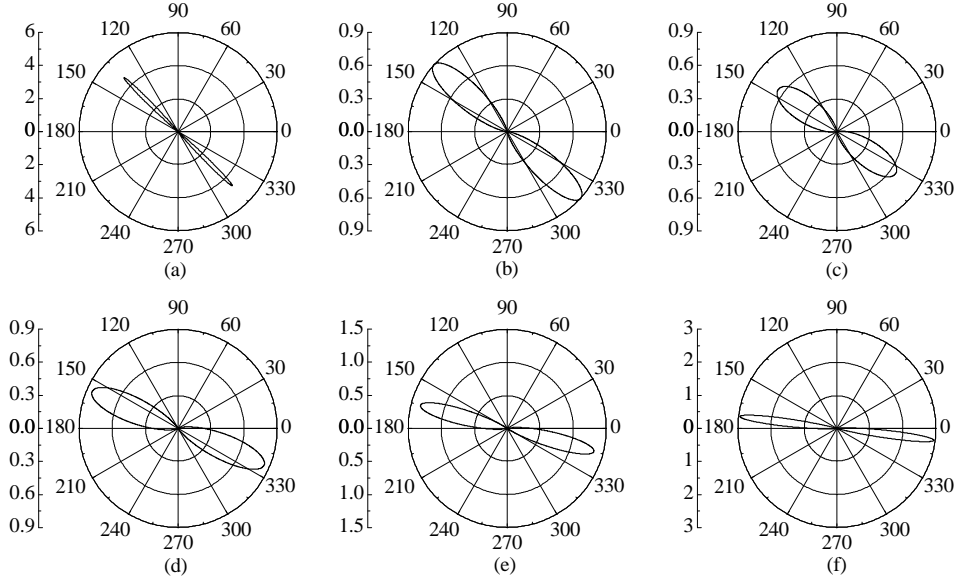


FIG. 5. Polar diagram of $\Phi(\varphi)$ for (a) $a = 0.354652$ ($\sigma = 10^5$), (b) $a = 0.442229$ ($\sigma = 10^2$), (c) $a = 0.708415$ ($\sigma = 10$), (d) $a = 2.485530$ ($\sigma = 2$), (e) $a = 10$ ($\sigma = 1.427204$), and (f) $a = 10^2$ ($\sigma = 1.282082$). Case (a) corresponds to a shear rate slightly larger than the threshold value $a_{\text{th}} \simeq 0.3520$, while case (f) corresponds to an exponent σ slightly larger than the minimum value $\sigma_{\min} \simeq 1.252$. Note that the scales in cases (a), (e), and (f) are different from the scales in cases (b)–(d).

V. CONCLUDING REMARKS

In this paper we have shown that the stationary solution of the (thermostatted) Boltzmann–Fokker–Planck equation for a two-dimensional gas of Maxwell molecules under uniform shear flow exhibits an algebraic high-velocity tail of the form given by Eq. (25), where $\sigma(a)$ is a decreasing function of the shear rate a . As a consequence, all the velocity moments of a degree equal to or larger than $2 + \sigma(a)$ diverge. The word “thermostat” does not mean in the present context that an external drag force is necessarily applied on the system; its effect for Maxwell molecules is equivalent to a rescaling of the velocities with respect to the thermal velocity and this is the point of view adopted in this paper. The restriction to an idealized scattering model with grazing collisions, Eq. (16), allows us to replace the complicated structure of the Boltzmann collision operator by a much more manageable Fokker–Planck operator, Eq. (17). This operator is formally linear in velocity space, but the original bilinear nature of the collision operator appears via the dependence of some of the coefficients on the distribution function through the pressure tensor. On the other hand, those nonlinear terms are negligible in the limit of large velocities and thus one arrives at a linear second-order ordinary differential equation for Φ , Eq. (30). Despite the linearity of the problem posed by Eq. (30), it applies to states arbitrarily far from equilibrium. As a matter of fact, the nonlinear nature of the underlying state is still present through the dependence of the “thermostat” (or scaling) parameter α on the shear rate a , Eq. (14). The structure of Eq. (30) is reminiscent of Mathieu’s equation; in fact the latter is obtained by formally setting the parameter $p = 0$, although this is not possible in the physical problem at hand. The symmetry property $f(\mathbf{V}) = f(-\mathbf{V})$ translates into the periodicity condition $\Phi(\varphi) = \Phi(\varphi + \pi)$. Enforcements of this condition on the solutions to Eq. (30) allows us to obtain $\sigma(a)$ from the solution of the continued fraction representation (41), the latter becoming an algebraic equation when $\sigma = 2, 4, 6, \dots$. The results show that $\sigma(a)$ is lower bounded by the value $\sigma_{\min} \simeq 1.252$ (which is asymptotically reached in the limit $a \rightarrow \infty$) and goes to infinity when the shear rate approaches the threshold value $a_{\text{th}} \simeq 0.352$ (in units of the collision frequency). The first property implies that all the moments of degree equal to or smaller than $2 + \sigma_{\min} \simeq 3.252$ are finite in the steady state, regardless of how large the shear rate is. As a consequence of the second property, there exists a window of shear rates $0 \leq a \leq a_{\text{th}}$ where the high-velocity population decays more rapidly than algebraically (e.g., as a stretched exponential), all the moments being finite. The lobular shape of the orientation distribution $\Phi(\varphi)$ [cf. Fig. 5] shows that the high-velocity population is highly anisotropic, a feature already observed in Monte Carlo simulations for the isotropic scattering model.¹³ Most of the particles having a large (peculiar) velocity \mathbf{V} move along a narrow bunch of directions around a preferred direction characterized by the (equivalent) angles $\tilde{\varphi}(a)$ and $\tilde{\varphi}(a) + \pi$. The angle $\tilde{\varphi}(a)$ rotates counter-clockwise from $\tilde{\varphi} = 3\pi/4$ (i.e., $V_y/V_x = -1$) at $a = a_{\text{th}}$ to $\tilde{\varphi} = \pi$ (i.e., $V_y/V_x \rightarrow 0^-$) in the limit $a \rightarrow \infty$. The width of the angular distribution is zero in both limits, being maximum at a shear rate $a \approx 1$.

It is worth remarking that, despite the simplicity and artificiality of the scattering model considered in this paper, it succeeds in capturing the most relevant features that were expected on the basis of Monte Carlo simulations and moment method results in the case of more realistic scattering laws:^{12,13} the existence of a high-velocity tail with a monotonically decreasing exponent $\sigma(a)$ and with a strongly anisotropic orientation distribution $\Phi(\varphi; a)$. Thus, the asymptotic behavior (25) is not an artifact of the specific model (17), but a general property of Maxwell molecules under uniform shear flow. Some other features, however, are possibly peculiar of the singular scattering law (16). For instance, the results of Ref. 13 for the isotropic scattering model seem to indicate that $\sigma(a)$ only diverges when $a \rightarrow 0$ (i.e., $a_{\text{th}} = 0$) and that $\lim_{a \rightarrow \infty} \sigma(a) = 0$ (i.e., $\sigma_{\min} = 0$). It is possible that the extreme anisotropy of the scattering model (16) makes the high-velocity tail phenomenon to be milder than in the general case, thus yielding non-zero values for a_{th} and σ_{\min} . On a different vein, it must be said that since the problem reduces to a linear equation, we have not determined either the coefficient measuring the amplitude of the tail (25) or the order of magnitude of the characteristic velocity c , such that (25) applies when $V \gg c$. Monte Carlo simulations¹³ show that the amplitude is a decreasing function of the shear rate, while c is rather insensitive to the shear rate. The value of c seems to be of the order of the thermal velocity $v_0 = \sqrt{2k_B T/m}$, so that the asymptotic behavior (25) is reached in practice for $V \gtrsim 10v_0$. The theoretical confirmation of both properties would require the analysis of the full kinetic equation (24) and this is beyond the scope of this work.

It must be remarked that in this paper we have considered the replacement (17) as a collision model by itself. On the other hand, it is known that the right-hand side of (17) actually represents the contribution to the true collision operator associated with grazing collisions.⁵ Therefore, it is tempting to conjecture that, in general, the high-velocity tail is produced by grazing collisions of high-velocity particles. Since the expansion leading to (17) is non-uniform for high velocities,⁵ the analysis of this paper does not provide a rigorous proof of the above conjecture but, at most, a strong indication of it.

The results presented in this paper, along with those of Refs. 10–14, show that the population of high energy levels in the uniform shear flow, and possibly in many other nonequilibrium states, is far greater than in the corresponding equilibrium state described by the Maxwell–Boltzmann distribution function. Among other examples of

nonequilibrium states exhibiting algebraic high-velocity tails we can mention the viscous longitudinal flow of Maxwell molecules²⁸ and the homogeneous cooling state of inelastic Maxwell molecules.²⁹ As a consequence of these nonequilibrium overpopulation effects, many more particles than at equilibrium can be available for surmounting the energy barriers of chemical and nuclear reactions which, consequently, would proceed faster. We also guess that fluctuations are enhanced with respect to the equilibrium ones, but the analysis of this expectation would require the treatment of the fluctuating Boltzmann equation.³⁰ This is an interesting avenue for further theoretical work.

ACKNOWLEDGMENTS

L.A. and A.S. acknowledge partial support from the Ministerio de Ciencia y Tecnología (Spain) through grant No. BFM2001-0718. This work was initiated while A.S. and A.V.B. were visiting the Department of Aeronautics and Astronautics, Graduate School of Engineering, Kyoto University, as visiting fellows of the Japan Society for the Promotion of Sciences. They are grateful to Profs. Y. Sone and K. Aoki for their kind hospitality.

APPENDIX A: DERIVATION OF EQ. (11)

The Boltzmann collision operator for Maxwell molecules is

$$Q[\mathbf{V}_1|f, f] = \int d\mathbf{V}_2 \int d\Omega K(\theta) [f(\mathbf{V}'_1)f(\mathbf{V}'_2) - f(\mathbf{V}_1)f(\mathbf{V}_2)], \quad (\text{A1})$$

where

$$\mathbf{V}'_1 = \mathbf{V}_1 - (\mathbf{g} \cdot \hat{\boldsymbol{\sigma}}) \hat{\boldsymbol{\sigma}}, \quad \mathbf{V}'_2 = \mathbf{V}_2 + (\mathbf{g} \cdot \hat{\boldsymbol{\sigma}}) \hat{\boldsymbol{\sigma}}. \quad (\text{A2})$$

Here, $\mathbf{g} \equiv \mathbf{V}_1 - \mathbf{V}_2$ is the relative velocity and $\hat{\boldsymbol{\sigma}}$ is a unit vector lying on the scattering plane and making an angle equal to $\frac{1}{2}(\pi - \theta)$ with the vector \mathbf{g} .

Given an arbitrary function $H(\mathbf{V}_1)$, standard manipulations yield

$$\int d\mathbf{V}_1 H(\mathbf{V}_1) Q[\mathbf{V}_1|f, f] = \frac{1}{2} \int d\mathbf{V}_1 \int d\mathbf{V}_2 \int d\Omega K(\theta) f(\mathbf{V}_1) f(\mathbf{V}_2) [H(\mathbf{V}'_1) + H(\mathbf{V}'_2) - H(\mathbf{V}_1) - H(\mathbf{V}_2)]. \quad (\text{A3})$$

In the particular case of $H(\mathbf{V}_1) = m\mathbf{V}_1\mathbf{V}_1$,

$$H(\mathbf{V}'_1) + H(\mathbf{V}'_2) - H(\mathbf{V}_1) - H(\mathbf{V}_2) = m(\mathbf{g} \cdot \hat{\boldsymbol{\sigma}}) [2(\mathbf{g} \cdot \hat{\boldsymbol{\sigma}}) \hat{\boldsymbol{\sigma}} \hat{\boldsymbol{\sigma}} - \hat{\boldsymbol{\sigma}} \mathbf{g} - \mathbf{g} \hat{\boldsymbol{\sigma}}]. \quad (\text{A4})$$

Taking into account the identities

$$\int d\Omega K(\theta) (\mathbf{g} \cdot \hat{\boldsymbol{\sigma}}) \hat{\boldsymbol{\sigma}} = B_1 \mathbf{g}, \quad (\text{A5})$$

$$\int d\Omega K(\theta) (\mathbf{g} \cdot \hat{\boldsymbol{\sigma}})^2 \hat{\boldsymbol{\sigma}} \hat{\boldsymbol{\sigma}} = B_2 \mathbf{g} \mathbf{g} - \frac{B_1 - B_2}{d-1} (\mathbf{g} \mathbf{g} - g^2 \mathbf{l}), \quad (\text{A6})$$

where \mathbf{l} is the $d \times d$ unit tensor and

$$B_k \equiv \int d\Omega K(\theta) \sin^{2k} \frac{\theta}{2}, \quad (\text{A7})$$

we finally have

$$\begin{aligned} \int d\mathbf{V}_1 m\mathbf{V}_1\mathbf{V}_1 Q[\mathbf{V}_1|f, f] &= -\frac{d}{d-1} (B_1 - B_2) \int d\mathbf{V}_1 \int d\mathbf{V}_2 f(\mathbf{V}_1) f(\mathbf{V}_2) m \left(\mathbf{g} \mathbf{g} - \frac{1}{d} g^2 \mathbf{l} \right) \\ &= -\frac{2d}{d-1} (B_1 - B_2) n (\mathbf{P} - p \mathbf{l}). \end{aligned} \quad (\text{A8})$$

This allows us to identify the effective collision frequency of Eq. (9) as $\nu = n(B_1 - B_2)2d/(d-1)$.

APPENDIX B: DERIVATION OF EQ. (17)

Let us start rewriting Eq. (A3) as

$$I[H] \equiv \int d\mathbf{V}_1 H(\mathbf{V}_1) Q[\mathbf{V}_1|f, f] = \int d\mathbf{V}_1 \int d\mathbf{V}_2 \int d\Omega K(\theta) f(\mathbf{V}_1) f(\mathbf{V}_2) [H(\mathbf{V}'_1) - H(\mathbf{V}_1)], \quad (\text{B1})$$

where $H(\mathbf{V}_1)$ is an arbitrary function. Now, according to the scattering law (16), $(\mathbf{g} \cdot \hat{\boldsymbol{\sigma}}) = g \sin(\epsilon/2)$, so that $\mathbf{V}'_1 - \mathbf{V}_1 \sim \epsilon$. This justifies the approximation

$$H(\mathbf{V}'_1) - H(\mathbf{V}_1) \simeq -\frac{\partial H(\mathbf{V}_1)}{\partial V_{1i}} (\mathbf{g} \cdot \hat{\boldsymbol{\sigma}}) \hat{\sigma}_i + \frac{1}{2} \frac{\partial^2 H(\mathbf{V}_1)}{\partial V_{1i} \partial V_{1j}} (\mathbf{g} \cdot \hat{\boldsymbol{\sigma}})^2 \hat{\sigma}_i \hat{\sigma}_j. \quad (\text{B2})$$

Consequently,

$$I[H] \rightarrow \int d\mathbf{V}_1 \int d\mathbf{V}_2 f(\mathbf{V}_1) f(\mathbf{V}_2) \left\{ -B_1 \frac{\partial H(\mathbf{V}_1)}{\partial V_{1i}} g_i + \frac{1}{2} \frac{\partial^2 H(\mathbf{V}_1)}{\partial V_{1i} \partial V_{1j}} \left[B_2 g_i g_j - \frac{B_1 - B_2}{d-1} (g_i g_j - g^2 \delta_{ij}) \right] \right\}, \quad (\text{B3})$$

where we have made use of (A5) and (A6). On the other hand, $\lim_{\epsilon \rightarrow 0} B_2 = 0$, while $B_1 \rightarrow (\nu/n)(d-1)/2d$ remains constant. Integrating over \mathbf{V}_2 in Eq. (B3), we have

$$I[H] \rightarrow \frac{d-1}{2d} \nu \int d\mathbf{V}_1 H(\mathbf{V}_1) \frac{\partial}{\partial V_{1i}} \left[V_{1i} - \frac{1}{2(d-1)} \frac{\partial}{\partial V_{1j}} \left(V_{1i} V_{1j} - V_1^2 \delta_{ij} + \frac{P_{ij} - dp \delta_{ij}}{mn} \right) \right] f(\mathbf{V}_1), \quad (\text{B4})$$

where we have integrated by parts. Since $H(\mathbf{V}_1)$ is arbitrary, it follows that

$$Q[\mathbf{V}_1|f, f] \rightarrow \frac{d-1}{4d} \nu \frac{\partial}{\partial V_{1i}} \left[V_{1i} + \frac{1}{d-1} \left(\frac{dp \delta_{ij} - P_{ij}}{mn} + V_1^2 \delta_{ij} - V_{1i} V_{1j} \right) \frac{\partial}{\partial V_{1j}} \right] f(\mathbf{V}_1), \quad (\text{B5})$$

- ¹ J. W. Dufty, J. J. Brey, and A. Santos, in *Molecular-Dynamics Simulation of Statistical-Mechanical Systems*, edited by G. Ciccotti and W. G. Hoover (North-Holland, Amsterdam, 1986), pp. 294–303.
- ² A. W. Lees and S. F. Edwards, *J. Phys. C* **5**, 1921 (1972).
- ³ J. M. Montanero, V. Garzó, and A. Santos, *Phys. Fluids* **12**, 3060 (2001).
- ⁴ A. Santos, V. Garzó, and J. J. Brey, *Phys. Rev. A* **46**, 8018 (1992).
- ⁵ C. Cercignani, *Theory and Application of the Boltzmann Equation* (Scottish Academic Press, Edinburgh, 1975).
- ⁶ C. Cercignani, *Mathematical Methods in Kinetic Theory* (Plenum Press, New York, 1990).
- ⁷ E. Ikenberry and C. Truesdell, *J. Rat. Mech. Anal.* **5**, 1 (1956).
- ⁸ C. Truesdell, *J. Rat. Mech. Anal.* **5**, 55 (1956).
- ⁹ C. Truesdell and R. G. Muncaster, *Fundamentals of Maxwell's Kinetic Theory of a Simple Monatomic Gas* (Academic Press, New York, 1980).
- ¹⁰ A. Santos and V. Garzó, *Physica A* **213**, 409 (1995).
- ¹¹ A. Santos, V. Garzó, J. J. Brey, and J. W. Dufty, *Phys. Rev. Lett.* **71**, 3971 (1993); **72**, 1392 (Erratum) (1994).
- ¹² J. M. Montanero, A. Santos, and V. Garzó, *Phys. Rev. E* **53**, 1269 (1996).
- ¹³ J. M. Montanero, A. Santos, and V. Garzó, *J. Stat. Phys.* **88**, 1165 (1997).
- ¹⁴ J. M. Montanero, V. Garzó, and A. Santos, in *Rarefied Gas Dynamics 20th*, edited by C. Shen (Peking University Press, Beijing, 1997), pp. 113–117.
- ¹⁵ J. R. Dorfman and H. van Beijeren, in *Statistical Mechanics, Part B*, edited by B. J. Berne (Plenum, New York, 1977), pp. 65–179.
- ¹⁶ J. W. Dufty, A. Santos, J. J. Brey, and R. F. Rodríguez, *Phys. Rev. A* **33**, 459 (1986).
- ¹⁷ C. Cercignani, *Transport Theory Stat. Phys.* **182**, 125 (1989).
- ¹⁸ C. Cercignani and S. Cortese, *J. Stat. Phys.* **75**, 817 (1994).
- ¹⁹ M. H. Ernst, *Phys. Rep.* **78**, 1 (1981).
- ²⁰ A. V. Bobylev, *Sov. Sci. Rev. C Math. Phys.* **7**, 111 (1988).
- ²¹ J. A. McLennan, *Introduction to Non-equilibrium Statistical Mechanics* (Prentice Hall, Englewood Cliffs, N. J., 1989).

- ²² J. M. Montanero, A. Santos, and V. Garzó, *Phys. Fluids* **8**, 1981 (1996).
- ²³ W. G. Hoover, *Ann. Rev. Phys. Chem.* **34**, 103 (1983).
- ²⁴ D. J. Evans and G. P. Morriss, *Comput. Phys. Rep.* **1**, 299 (1984).
- ²⁵ D. J. Evans and G. P. Morriss, *Statistical Mechanics of Nonequilibrium Liquids* (Academic Press, London, 1990).
- ²⁶ *Handbook of Mathematical Functions*, edited by M. Abramowitz and I. A. Stegun (Dover, New York, 1972), Ch. 20.
- ²⁷ *Table of Integrals, Series and Products*, edited by I. S. Gradshteyn and I. M. Ryzhik (Academic Press, New York, 1965), Ch. 8.6.
- ²⁸ A. Santos, *Phys. Rev. E* **62**, 6597 (2000) and cond-mat/0002240.
- ²⁹ P. L. Krapivsky and E. Ben-Naim, *J. Phys. A: Math. Gen.* **35**, L147 (2002); A. Baldassarri, U. Marini Bettolo Marconi, and A. Puglisi, *Europhys. Lett.* **58**, 14 (2002); M. H. Ernst and R. Brito, *Europhys. Lett.* **58**, 182 (2002).
- ³⁰ E. G. D. Cohen, in *Fundamental Problems in Statistical Mechanics V*, edited by E. G. D. Cohen (North-Holland, Amsterdam, 1980), pp. 235–248.